

Precisely tunable continuous-wave terahertz source with interferometric frequency control

Anselm J. Deninger, Thorsten Göbel, Daniel Schönherr, Thomas Kinder, Axel Roggenbuck, Markus Köberle, Frank Lison, Thomas Müller-Wirts, and Peter Meissner

TOPTICA Photonics AG, Lochhamer Schlag 19, D-82166 Gräfelfing, Germany; Hochfrequenztechnik, Technische Universität Darmstadt, Merckstrasse 25, D-64283 Darmstadt, Germany; and TEM Messtechnik GmbH, Grosser Hillen 38, D-30559 Hannover, Germany

(Received 7 February 2008; accepted 13 March 2008; published online 15 April 2008)

We realized a tunable continuous-wave terahertz source with megahertz frequency resolution. The system is based on optical heterodyning of two near-infrared distributed feedback diode lasers, each laser being stabilized by electronic feedback from a low-finesse quadrature interferometer. The control loop permits precisely linear laser frequency scans over >1200 GHz, and a beat signal linewidth of 1 MHz at 80 ms time scale. Using GaAs photomixers and log-periodic antennae, we achieve a signal-to-noise ratio of the terahertz power of >70 dB at 100 GHz and 100 ms integration time, and still ~ 30 dB at 1 THz. As an example for high-resolution terahertz spectroscopy, we characterize the transmission properties of a subwavelength metal grating. © 2008 American Institute of Physics. [DOI: [10.1063/1.2905033](https://doi.org/10.1063/1.2905033)]

I. INTRODUCTION

Terahertz radiation bears great potential in imaging and spectroscopy alike, with fields of application ranging from material inspection to the analysis of foodstuffs, chemical process control, and security technology.¹ It is well known that the spectral resolution attainable with a continuous-wave (cw) terahertz source is superior to a broadband pulsed emitter. Direct electronic generation of cw terahertz radiation offers high power levels in the mW range,² but as yet limited, if any, frequency tuning. On the other hand, wide tuning ranges, although at the cost of terahertz intensity, are realized with optoelectronic techniques. One of the established methods of generating tunable cw terahertz light is optical heterodyning:³ an interleaved metal-semiconductor-metal structure (“photomixer”) is irradiated with two near-infrared (NIR) lasers of adjacent wavelengths, and a resonant antenna surrounding the photomixer emits an electromagnetic wave at the terahertz difference frequency. Benefits of this technique are a very wide bandwidth, low initial and operating costs, and simple implementation.

Within the past few years, NIR distributed feedback (DFB) lasers have become commercially available and been successfully used both for cw terahertz imaging and spectroscopy.^{4,5} DFB diodes feature a grating structure within the active region of the semiconductor, restricting their emission spectrum to a single longitudinal mode. Varying the grating pitch either thermally or electrically tunes the lasing wavelength, and continuous frequency scans of >1000 GHz can be realized by means of a temperature sweep of ~ 40 K.

The attainable frequency resolution of a cw terahertz setup is only limited by the frequency stability and linewidth of the utilized laser sources. However, the sensitivity of the DFB wavelength to changes of the chip current or

temperature—the very effect responsible for the large tuning range—makes the DFB laser susceptible to frequency jitter and drifts. Without active frequency control, this results in a technical linewidth of ~ 5 MHz on a time scale of 100 ms, while the drift can be as high as several 100 MHz within few minutes. For high-resolution terahertz spectroscopy, this is clearly not sufficient.

We developed a tunable cw terahertz source, which combines 855 nm DFB diode technology and precise interferometric frequency control. Electronic feedback from a low-finesse Fabry–Pérot etalon serves to stabilize the laser frequency to arbitrary values within the diode’s tuning range, achieving a frequency resolution on the 1 MHz level. The laser frequency remains actively controlled even during a scan, enabling precisely linear ramps of the terahertz difference frequency. The entire laser setup is based on fiber optics, the optical beat signal being transmitted to the photoconductive chips via single-mode fibers.

In this report, we first describe the laser source, the interferometer concept used for frequency control, and the terahertz setup. We discuss the spectral resolution of the system, and show measurements of the beat signal mixing efficiency and the terahertz signal-to-noise ratio (SNR). As an application example, we present a high-resolution measurement of the transmission spectrum of a subwavelength metal grating, and compare the result to an analytical model.

II. EXPERIMENTAL DESIGN

A. Laser source

Our terahertz source employs two DFB lasers (Toptica DL DFB) with center wavelength of 855 nm. The maximum output power per laser is 130 mW. The utilized diodes were screened for large continuous tuning ranges (>1000 GHz over a 40–45 K temperature sweep).

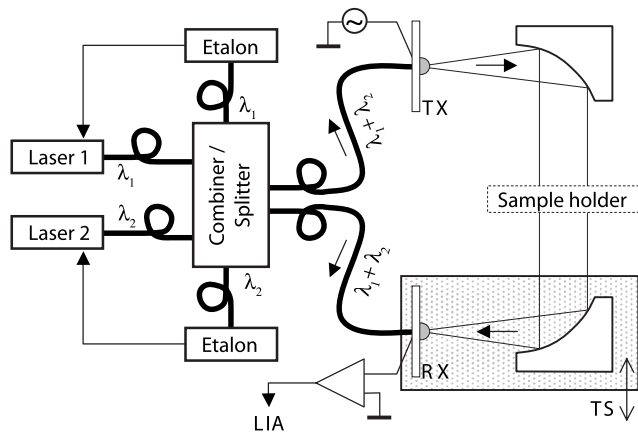


FIG. 1. Experimental setup (see text for explanations). TX is the transmitter, RX is the receiver, TS is the translation stage, and LIA is the lock-in amplifier.

Each DFB laser is protected from optical feedback by a 60 dB isolator, and coupled into a fiber array made of single mode, polarization-maintaining Panda fiber. From each input, a fiber tap (Fig. 1) extracts approximately 1% of the guided light intensity. The tap output is used in the frequency and power control loops of the respective laser (see below). The main beams are mixed in a 2×2 fiber combiner, and the two outputs carrying the beat signal are connected to the terahertz transmitter and receiver, respectively. Compared to conventional cw terahertz systems, the all-fiber setup considerably improves the flexibility and power stability.

B. Interferometric frequency control

For frequency stabilization as well as controlled frequency tuning, each DFB laser is regulated by electronic feedback from a fiber-coupled quadrature interferometer (Fig. 2).⁶ A wedge shaped beam splitter within the interferometer head generates two low-intensity probe beams (PB_A and PB_B), which enter a low-finesse, temperature-stabilized Fabry-Pérot etalon (free spectral range of 7.7 GHz) under slightly different angles. The etalon generates a pair of interference signals with a relative phase of $\pi/2$. These signals are detected by two photodiodes (a, b) and combined into a quadrature signal, the phase of which is a linear function of the optical frequency.

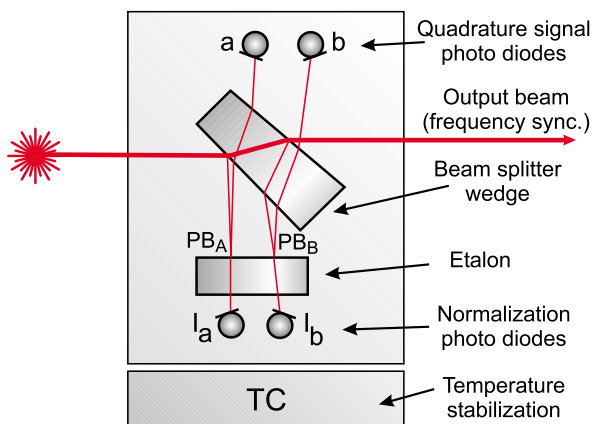


FIG. 2. (Color online) Quadrature interferometer.

The interferometrically measured phase is compared to a microprocessor-computed set-point phase representing the user-selected target frequency. The resulting error signal is processed by a proportional-integral-derivative regulator and fed back to both temperature and current of the DFB laser. For small frequency steps (< 3 GHz), the laser frequency adapts the set-point value within less than 0.5 ms. Frequency fluctuations due to thermal drifts or electronic jitter are thus eliminated. The resolution of this frequency control loop is approximately $1/10\,000$ of the etalon free spectral range, i.e., on the 1 MHz level.

Two further photodiodes within the quadrature interferometer (labeled I_a, I_b in Fig. 2) serve to monitor the laser intensity. The intensity value is used in an additional control loop that corrects the laser current in order to maintain a constant average output power over the entire tuning range of the DFB laser.

In our terahertz experiment, the laser beams transmitted through the respective interferometer (“output beam” in Fig. 2) are combined on a fast photodetector, which synchronizes the two interferometers (measurement of frequency difference $\Delta\nu=0$). Both quadrature interferometers are controlled via a standard PC with serial interface.

C. Terahertz setup

The terahertz transmitter and receiver chips, fabricated and mounted at TU Darmstadt, consist of low temperature grown (LTG) GaAs finger photomixers. The chip that supports the planar finger structure comprises a $350\ \mu\text{m}$ semi-insulating GaAs substrate, a 100 nm GaAs buffer layer, and a 400 nm $\text{Al}_{0.4}\text{Ga}_{0.6}\text{As}$ layer. This particular layer design was chosen for the possibility of having an etch stop. The 600 nm LTG-GaAs layer was grown in a molecular-beam-epitaxy facility (Riber 32) at an extrapolated substrate temperature of about $166\ ^\circ\text{C}$. After growing, it was annealed *ex situ* at a temperature of $600\ ^\circ\text{C}$ for 10 min.

Each photomixer is integrated within a log-periodic antenna and the terahertz signal is coupled into space via an attached silicon lens.⁷ The emitted terahertz beam is collimated by a parabolic mirror (focal length of 75 mm) and focused onto the receiver by a second, identical mirror.

Our setup employs a coherent detection scheme: the terahertz beam and the two-color laser beam are superimposed on the receiver, which generates a direct current proportional to the electric field of the terahertz wave, and to $\cos(2\pi fd/c)$, where f is the difference frequency of the lasers, d is the path length difference of pump and probe signal, and c is the speed of light. Changing the terahertz path length thus permits measurements of both field strength and phase of the terahertz wave. In our design, the terahertz transmitter and the first mirror are mounted on a rail, allowing a parallel shift driven by a step motor and hence, a length variation of the collimated terahertz beam path (cf. Fig. 1). This simple implementation of a variable delay line is enabled by the all-fiber-based system design in the first place.

Terahertz data acquisition is accomplished using lock-in detection techniques. To this end, the bias voltage of the transmitting log-periodic antenna is modulated at 220 Hz (modulation amplitude ± 10 V). The photocurrent of the re-

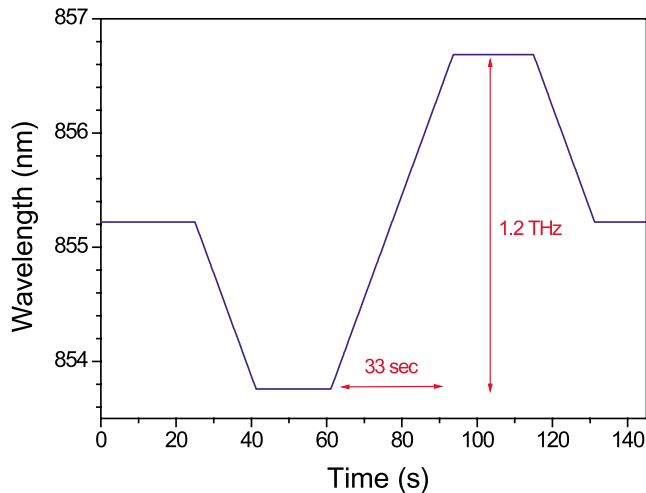


FIG. 3. (Color online) Tuning curve of a DFB laser with quadrature interferometer for frequency control. A linear scan of +0.6 THz is followed by a ramp of -1.2 THz, before the frequency returns to its initial value.

ceiver is fed, via a transimpedance amplifier, to a lock-in amplifier with a time constant of 100 ms. The electronic chopping was found to induce less noise in the terahertz signal than a mechanical chopper wheel. Thus, besides the step motor, no moving parts are included in the system, which increases the reliability and flexibility.

III. RESULTS AND DISCUSSION

A. Laser frequency and power stabilization

The tuning characteristics of the DFB lasers were measured with a high-resolution wavelength meter (HighFinesse-Angstrom WS/7). In total, eight DFB diodes emitting at 855 nm were examined, and thermal tuning coefficients between 24.9 and 27.5 GHz/K were measured. These values are in good agreement with previously reported thermal tuning coefficients of near-infrared DFB diodes (25 GHz/K).⁸

Over a temperature span of 3–48 °C, the above values translate into continuous frequency tuning ranges between 1120 and 1237 GHz. The temperature interval was chosen to match the working range of the utilized temperature controllers (0–50 °C).

Figure 3 shows a representative frequency tuning curve of a DFB laser with interferometric frequency control. In closed-loop operation, a precisely linear frequency scan over 1200 GHz was realized. In the example, the scan was composed of individual frequency steps of 10 MHz width. Each step was addressed with ~ 1 MHz precision within < 300 μ s, resulting in a total sweep time of 33 s.

Figure 4 depicts the relative power change during a 1000 GHz scan with, and without, the power control loop. Without active power regulation, the temperature is varied in a linear manner, and the laser current is used to correct the laser frequency in order to maintain a linear progression of frequency steps. This results, however, in strong power changes (up to a factor of 7), caused by beam pointing drifts that reduce the fiber coupling efficiency, and an overall decrease of the output power at elevated temperatures (frequency shift ~ 0 in the example).

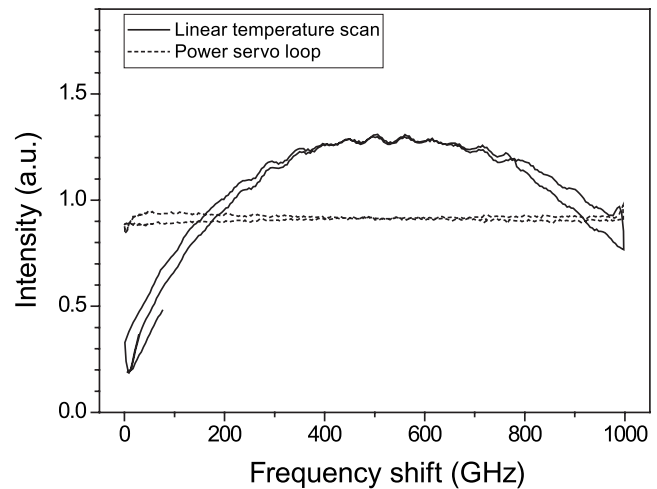


FIG. 4. Relative power variation during a 1000 GHz scan of the laser frequency. Solid line: linear frequency scan without power control; dotted line: scan with additional power control loop.

The power servo loop reduces the intensity variation to $\pm 7.2\%$ relative to the mean value. The residual power modulation is due to the delayed response of the laser temperature. Hence, the largest deviations occur at the turning points of the scan. Allowing a settling time of the laser frequency of approximately 5 s reduces the residual power deviation to a negligible value ($< 0.15\%$).

By combining two DFB lasers, a continuously tunable difference frequency from 0 to 1100–1200 GHz could be realized, with the upper limit depending on the utilized diodes. Optical beat measurements were performed at near-equal frequencies in order to assess the linewidth of the difference frequency signal and hence, terahertz wave (Fig. 5). The beat signal was sampled with 10 ns resolution using a digital oscilloscope with 500 MHz bandwidth (LeCroy WaveRunner 6050). At integration times as long as 80 ms, a beat full width at half maximum (FWHM) of ~ 1 MHz was measured. The signal exhibited a Gaussian waveform, from which we deduce a DFB laser linewidth of ~ 700 kHz.

As can be seen in Fig. 6, the beat linewidth of the

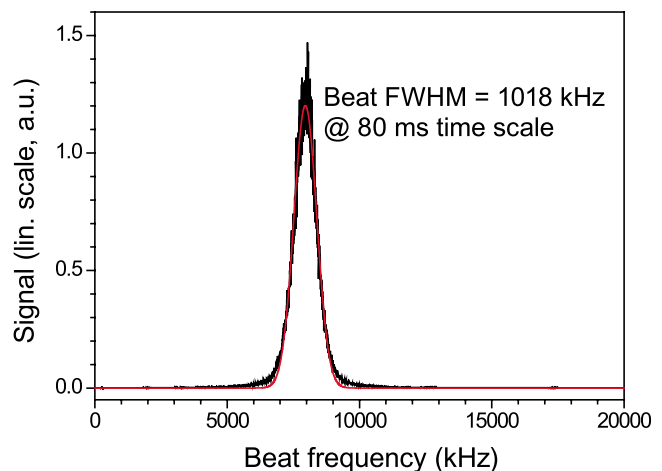


FIG. 5. (Color online) Beat signal of two lasers, each locked to a quadrature interferometer. A Lorentzian fit yields a FWHM beat linewidth of 1.0 MHz at a time scale of 80 ms.

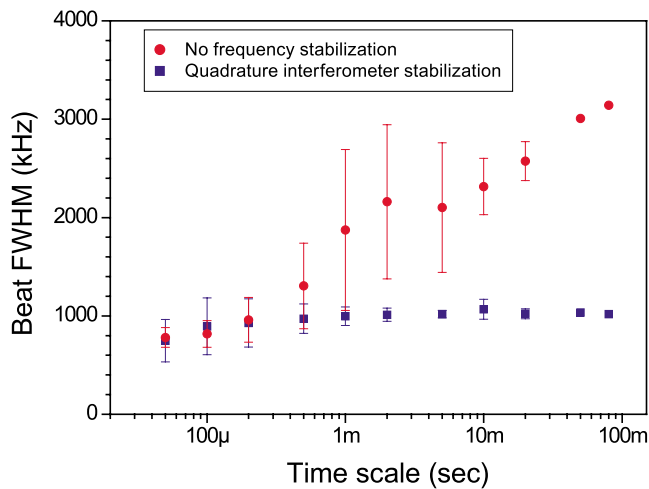


FIG. 6. (Color online) Beat signal linewidth of two DFB lasers with and without frequency stabilization, for time scales of $50 \mu\text{s}$ – 80 ms . The measurement was performed by dividing a data string of 80 ms , sampled at 100 MHz , into subintervals of different lengths. Symbols and error bars denote the mean and standard deviation of the results obtained for the subintervals. Data points at 50 and 80 ms have no error bars as they represent only a single measurement.

frequency-stabilized lasers remains near constant for time intervals $>500 \mu\text{s}$, i.e., there is no further line broadening on the millisecond scale. This is a noticeable difference compared to the unregulated lasers, where the beat FWHM amounts to $>3 \text{ MHz}$ already at 80 ms integration time. Figure 6 further shows that the beat signal of regulated and unregulated lasers is identical at time scales below $500 \mu\text{s}$, consistent with the regulator bandwidth of approximately 2 kHz .

By analyzing the beat signal before and after a 24 h measurement run, a long-term frequency stability better than 20 MHz at 24 h could be inferred.

To assess the quality of the beat signal, we measured the mixing efficiency of the two fiber outputs leading to the transmitter and receiver antenna, respectively. A scanning autocorrelator (APE Mini NIR) was employed to heterodyne the optical beat signal of each fiber with itself. Altering the phase difference between both components yielded a signal with modulated amplitude, the modulation depth of which coincides with the one of the optical beat signal.

Within a range from 100 to 1000 GHz , near-constant values of approximately 95% in one channel and 90% in the second channel were obtained (Fig. 7). The difference, and deviation from 100% , results from slightly different split ratios of the fiber-optic array. Still, according to our experience, the above mixing efficiencies are far superior to those attainable with free-beam optics.

B. Terahertz measurements

The tuning range of the terahertz signal was similar to the difference frequency range of the lasers, with a lower frequency limit of approximately 80 GHz resulting from the design of the utilized antennae.

In order to determine the SNR characteristics of the terahertz signal, the difference frequency was varied from 100 to 1100 GHz in steps of 10 GHz . For each frequency

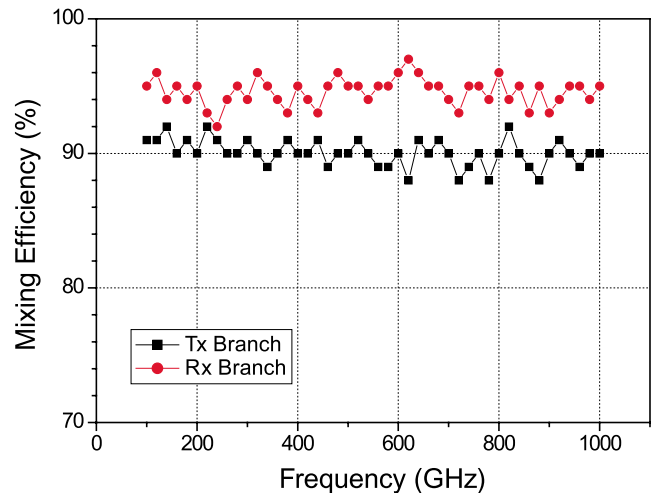


FIG. 7. (Color online) Mixing efficiency of the two-color beat signal for frequencies from 100 to 1000 GHz .

step, the phase between the terahertz signal and the optical beat at the receiver was equalized via the mechanical delay stage, and the receiver photocurrent was measured. The lock-in time constant was set to 100 ms . The noise level was determined by blocking the terahertz beam at the receiver, with otherwise identical settings. The average noise floor was $29 \pm 3 \text{ pA}$.

As evident from Fig. 8, SNR levels of the terahertz power above 70 dB were attained at frequencies around 100 GHz . This corresponds to an absolute amplitude of the photocurrent of $>110 \text{ nA}$ and a terahertz power of $\sim 200 \text{ nW}$ (confirmed with a Schottky detector from ACST GmbH, Germany, that was calibrated with a Golay cell). The reduced SNR toward higher frequencies mirrors the decrease of the photomixer efficiency (-40 dB/decade). The “dips” seen, e.g., at 120 , 160 , 240 , and 330 GHz are a result of the log-periodic design of the antenna and occur at frequencies that sit between the resonances of two adjacent antenna “arms.” These minima correspond to the minima of the an-

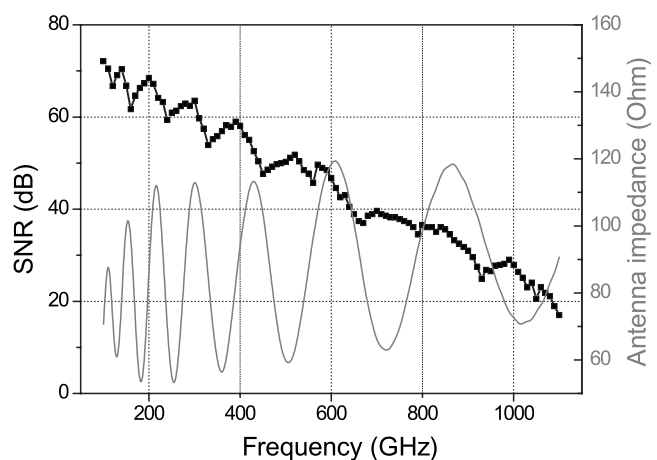


FIG. 8. Signal-to-noise performance of the terahertz system. The SNR value is computed by $20 \log(I_p/I_{\text{noise}})$, where I_p denotes the receiver photocurrent at a given terahertz frequency (mean value of 50 individual measurements), and I_{noise} is the mean noise floor (measured with blocked beam). The optical power at the transmitter was $2 \times 19 \text{ mW}$. The simulated antenna impedance is shown for comparison.

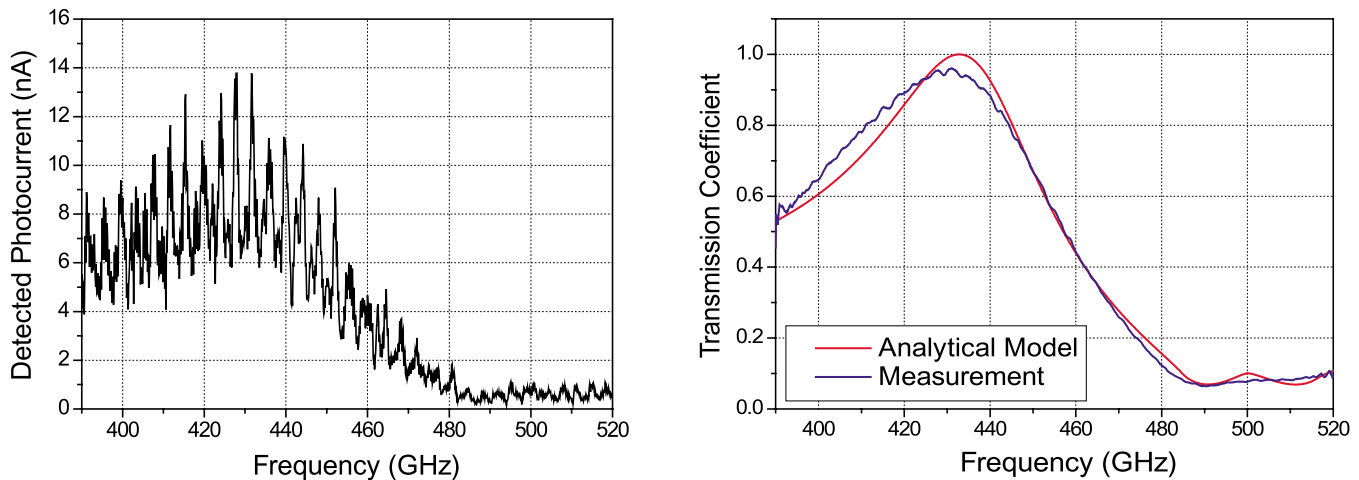


FIG. 9. (Color online) Transmission measurement of a subwavelength grating. Left: measured transmission spectrum without normalization to the free-space reference. Right: normalized transmission coefficient. In the analytical model, the grating is assumed to be perfectly conducting.

tenna impedance, a simulation (CST Microwave Studio) of which is also shown in Fig. 8. The maxima and minima of the simulation appear slightly blueshifted as compared to the actual measurement. This is attributed to the fact, that the effective permittivity of the antenna substrate, i.e., the LTG-GaAs layer on bulk GaAs, is not exactly known. Hence, the permittivity of bulk GaAs ($\epsilon=12.9$) was assumed for the simulation and we forgo further fitting for better agreement. The SNR curve further shows the prominent water vapor absorption line at 560 GHz.

C. Application example: Terahertz spectroscopy using subwavelength gratings

Metal films with periodic, subwavelength perforations feature remarkable transmission properties. On the one hand, they exhibit narrow, highly resonant optical and terahertz transmission peaks, whereas, on the other hand, zero transmission points can be monitored.⁹ Even though the nature of these extraordinary transmission attributes is still under discussion,¹⁰ several applications such as material characterization¹¹ or near field microscopy¹² have been proposed.

To date, almost all research into the transmission properties of subwavelength gratings has been performed with pulsed time-domain measurements, and results are therefore limited in accuracy. Using the cw terahertz system introduced above, the resolution can be improved by several orders of magnitude.

For a feasibility experiment, a grating featuring 70 periods of 600 μm each, a thickness of 200 μm , and a slit width of 100 μm was fabricated. Tombac, a copper/zinc alloy, was used as material because of its high rigidity. After a free-space reference measurement, the sample, mounted on a fiber glass frame, was placed in the collimated part of the terahertz beam, and the transmission spectrum was recorded in steps of 100 MHz.

As illustrated in Fig. 9, the received signal is superimposed by multiple periodic oscillations of different frequencies. They are caused by standing waves that evolve, e.g., between the grating and transmitter, or transmitter and re-

ceiver. This illustrates that not only a high frequency stability but also an exact adjustment of the absolute frequency is required: without precise frequency control, the measurement cannot be normalized to the free-space reference, leading to large errors.

After normalizing the recorded data to the free-space reference, the signal was gated in time domain to eliminate further reflections.¹³ For analytical modeling, we used a modal expansion approach to calculate the theoretical transmission coefficient for a perfectly conducting grating.¹⁴ As Fig. 9 shows, the obtained transmission spectrum is in excellent agreement with the theoretical prediction.

Potentially, these structures can be used both as narrow terahertz filters and as material sensors.¹⁵ Ongoing research has indicated that the spectral signatures of Fig. 9 appear redshifted when material layers are attached to the grating. It has already been demonstrated that in the gigahertz range, the permittivity of the sandwiching layers can be extracted from these redshift measurements.¹⁶ Furthermore, the high frequency resolution of the implemented system will allow the design and experimental verification of subwavelength gratings featuring much higher Q factors than that of our sample. Hence, the designed setup in combination with the grating sensors will enable precise material characterization within the terahertz spectral range.

In conclusion, we have realized an all-fiber-based cw terahertz system, which is superior to standard photoconductive terahertz setups in terms of flexibility and stability. Combining widely tunable DFB diode lasers and interferometric frequency control, we achieve a highly stable terahertz signal, with a frequency resolution on the 1 MHz level. This is, to our knowledge, the highest reported frequency resolution of tunable cw terahertz systems based on optical heterodyning. Further, the linear 1200 GHz scan of the frequency-controlled laser likely represents the largest frequency scan of a diode laser with megahertz precision.

In the system described here, the accessible range of terahertz difference frequencies was limited to 1200 GHz by the tuning ranges of the utilized laser diodes. Perspectively, the combination of two diodes with optimized frequency off-

set should double the terahertz tuning range. The interferometric stabilization technique would even work for lasers with non-matching frequencies (e.g., difference tuning from 0.5 to 2.5 THz), as each laser is individually regulated with high precision. In this case, however, a technique other than beat signal detection would be required for frequency synchronization. One possibility is the use of a terahertz absorption line for absolute frequency calibration.

Potential applications of a widely tunable, yet accurately adjustable cw terahertz source include high-resolution spectroscopy, e.g., of low-pressure gas samples, and material characterization, based on the assessment of the dielectric properties of foils or thin films attached to reference gratings or terahertz etalons.

ACKNOWLEDGMENTS

We thank Dr. Torsten Löffler (University of Frankfurt) and Gunter Feiss (TOPTICA Photonics) for experimental support and fruitful discussions. A.D., A.R., and F.L. further acknowledge funding by the German Research Ministry BMBF (“Lynkeus” project, FSK 16SV2304). T.G. acknowledges funding by the German Research Foundation (DFG) within the research training group “TICMO” (GRK 1037).

- ¹M. Tonouchi, *Nat. Photonics* **1**, 97 (2007).
- ²T. Löffler, T. May, C. am Weg, A. Alcin, B. Hils, and H. G. Roskos, *Appl. Phys. Lett.* **90**, 091111 (2007).
- ³K. A. McIntosh, E. R. Brown, K. B. Nichols, O. B. McMahon, W. F. di Natale, and T. M. Lyszczarz, *Appl. Phys. Lett.* **67**, 3844 (1995).
- ⁴R. Wilk, Ph.D. thesis, University of Braunschweig, 2007.
- ⁵I. S. Gregory, M. J. Evans, H. Page, S. Malik, I. Farrer, and H. E. Beere, *Appl. Phys. Lett.* **91**, 154103 (2007).
- ⁶Th. Müller-Wirts, U.S. Patent No. 6,178,002 (Jan. 23, 2001).
- ⁷R. Mendis, C. Sydlo, J. Sigmund, M. Feiginov, P. Meissner, and H. L. Hartnagel, *IEEE Antennas Wireless Propag. Lett.* **4**, 85 (2005).
- ⁸S. Kraft, A. Deninger, C. Trüick, J. Fortágh, F. Lison, and C. Zimmermann, *Laser Phys. Lett.* **2**, 71 (2005).
- ⁹T. W. Ebbesen, H. J. Lezec, H. F. Ghaemi, T. Thio, and P. A. Wolff, *Nature (London)* **391**, 667 (1998).
- ¹⁰N. Garcia and M. Nieto-Vesperinas, *J. Opt. A, Pure Appl. Opt.* **9**, 490 (2007).
- ¹¹F. Miyamaru, S. Hayashi, C. Otani, K. Kawase, and E. Kato, *Opt. Lett.* **31**, 1118 (2006).
- ¹²A. J. Ward and J. B. Pendry, *J. Mod. Opt.* **44**, 1703 (1997).
- ¹³G. A. Burrell and A. R. Jamieson, *IEEE Trans. Antennas Propag.* **21**, 702 (1973).
- ¹⁴Ph. Lalanne, J. P. Hugonin, S. Astilean, M. Palamaru, and K. D. Möller, *J. Opt. A, Pure Appl. Opt.* **2**, 48 (2000).
- ¹⁵T. Göbel, D. Schönherr, M. Feiginov, P. Meissner, and H. L. Hartnagel, *European Conference on Laser and Electro-Optics (CLEO Europe)*, Munich, Germany, 2007, edited by A. Ouarab (EPS, Mulhouse, 2007), Paper No. CH 2-2-MON.
- ¹⁶T. Göbel, D. Schönherr, C. Sydlo, M. Feiginov, P. Meissner, and H. L. Hartnagel, Proceedings of the Joint 32th International Conference on Infrared and Millimeter Waves and 12th International Conference Terahertz Electronics (IRMMW), Cardiff, UK, 2007, edited by M. J. Griffin (unpublished).